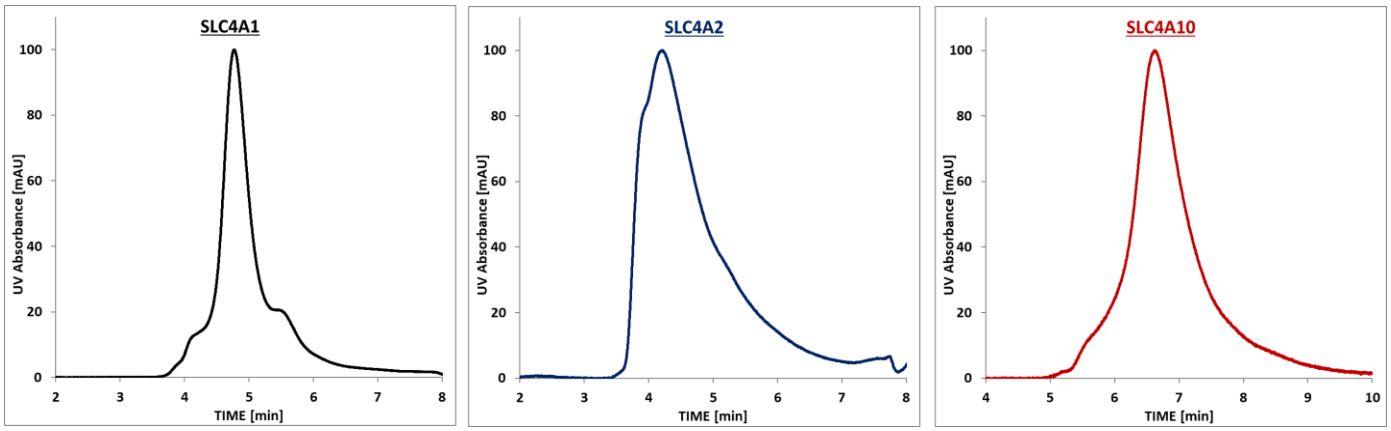

Figure 1 | Purification of full length human SLC4 transporters from insect cells. Monodisperse analytical size exclusion chromatograms show homogenous protein species for SLC4A1, SLC4A2, and SLC4A10 purified from insect cells.

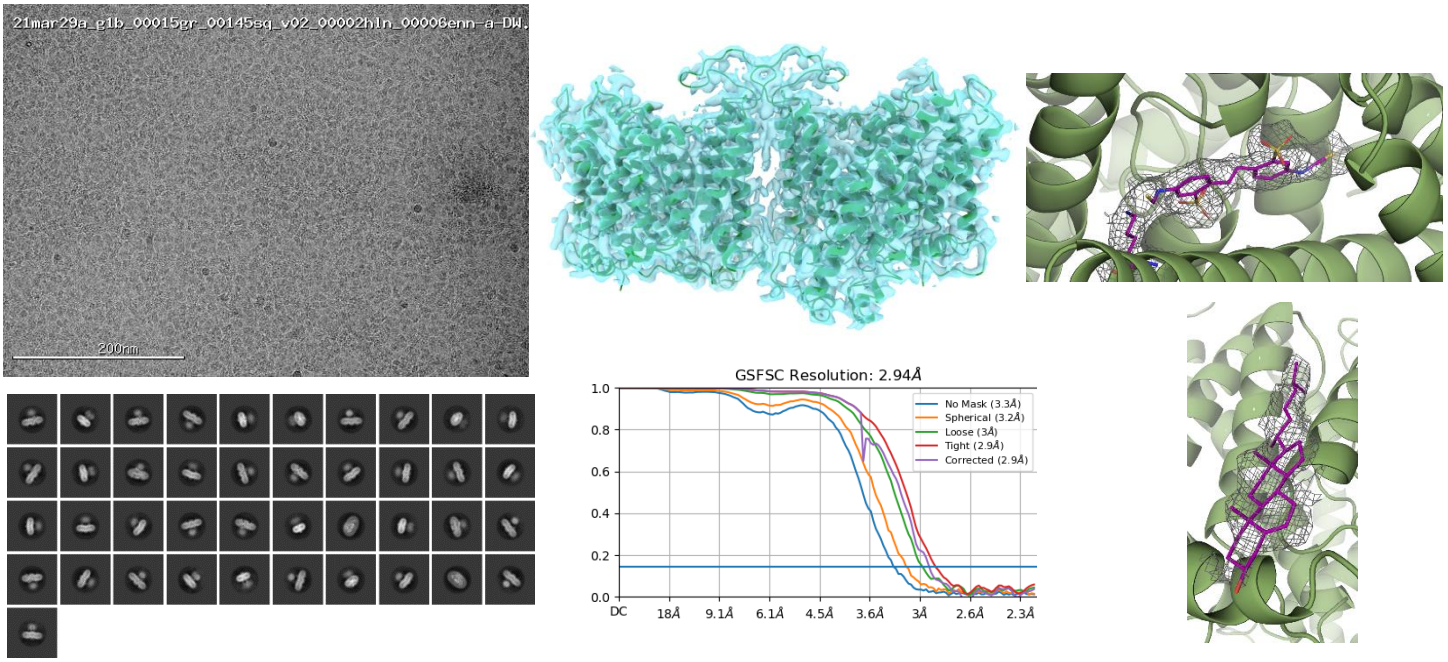

Figure 2 | Preliminary cryoEM data collection and SPA structure of full length human SLC4A1. Top Left, cryoEM micrograph of full length human SLC4A1 in detergent. **Bottom Left**, representative 2D classes showing SLC4A1 transmembrane domain and intracellular domain. **Top Middle**, sharpened cryoEM density and cartoon model of refined SLC4A1 transmembrane domain structure. **Bottom Middle**, FSC plot of cryosparc refinement indicating global resolution of 2.94 Angstrom. **Top Right**, SLC4A1 inhibitor stick model built into cryoEM density. **Bottom Right**, Cholesterol stick model built into cryoEM density.

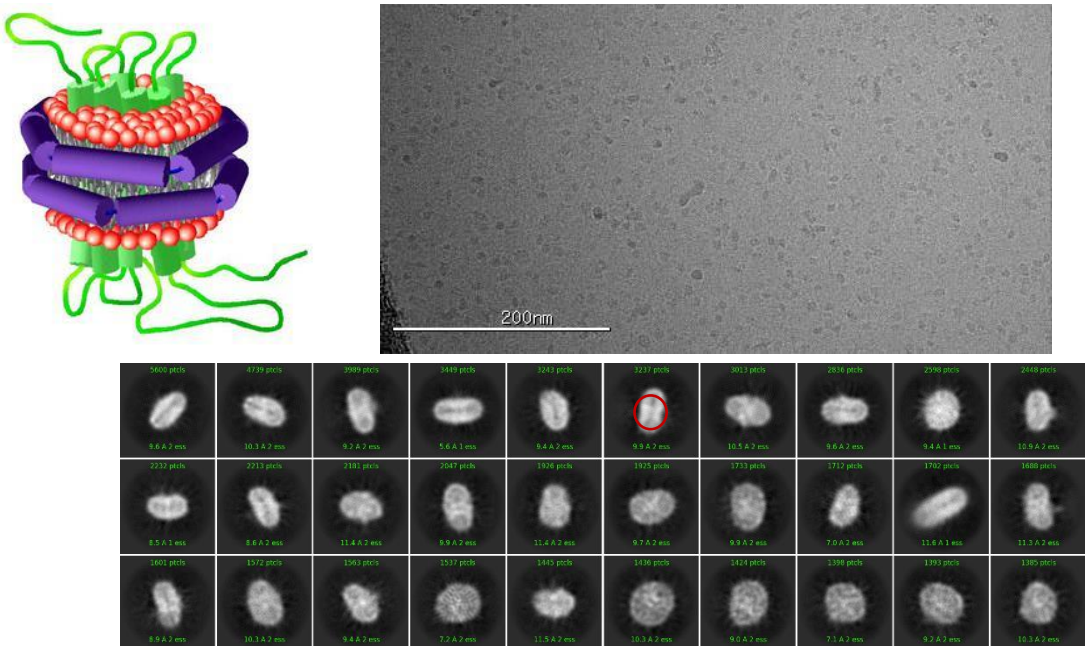

Figure 3 | Preliminary CryoEM data of SLC18A2/VMAT2-Nanodiscs. Top Left, schematic of nanodiscs containing membrane proteins (green), encased by lipids (red) and a belt protein (purple). **Top Right**, cryoEM micrograph of SLC18A2/VMAT2-nanodiscs on grids. **Bottom**, 2D class averages of particles show nanodisc shape, with clear transporter density inside (red circle).

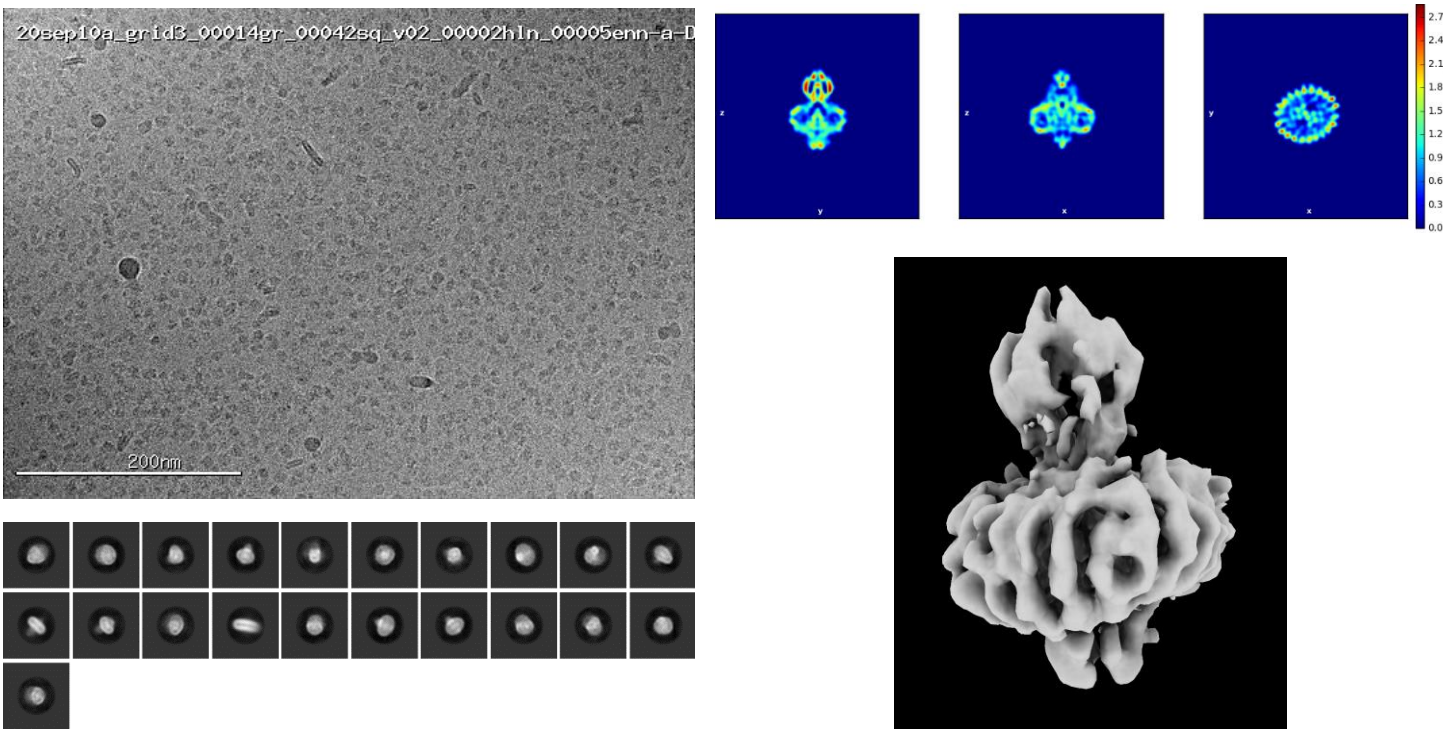

Figure 4 | Preliminary CryoEM data of SLC30A1/ZnT1-nanodiscs. Top Left, Representative cryoEM micrograph of SLC30A1/ZnT1-nanodiscs on grids. **Bottom Left**, 2D class averages of particles show nanodisc shape, with SLC30A1/ZnT1 density on either side of the nanodisc. **Top Right**, Sections of initial SLC30A1/ZnT1-nanodisc 3D reconstruction at around 6-8 Angstrom shown on **Bottom Right**.